Extraction and Analysis of RPE later from OCT Images for Detection of Age Related Macular Degeneration

Author

Muhammad Majid Sharif

NUST201464094MSEECS61314F

Supervisor

Dr. Asad Waqar Malik

DEPARTMENT OF COMPUTER

SCHOOL OF ELECTRICAL ENGINEERING AND COMPUTER SCIENCE

NATIONAL UNIVERSITY OF SCIENCES AND TECHNOLOGY

ISLAMABAD

May, 2018

Extraction and Analysis of RPE later from OCT Images for Detection of Age Related Macular Degeneration

Author

Muhammad Majid Sharif

NUST201464094MSEECS61314F

A thesis submitted in partial fulfillment of the Requirements for the degree of

MS Computer Science

Thesis Supervisor:

Dr. Asad Waqar Malik

Thesis Supervisor's Signature:_____

DEPARTMENT OF COMPUTER

SCHOOL OF ELECTRICAL ENGINEERING AND COMPUTER SCIENCE

NATIONAL UNIVERSITY OF SCIENCES AND TECHNOLOGY

ISLAMABAD

May, 2018

Approval

It is certified that the contents of thesis document titled "**Extraction and Analysis of RPE later from OCT Images for Detection of Age Related Macular Degeneration**" submitted by Mr. **Muhammad Majid Sharif** have been found satisfactory for the requirement of degree.

Advisor: **Dr. Asad Waqar Malik**

Signature: _____

Committee Member1: **Dr. Muhammad Usman Akram**

Signature: _____

Committee Member2: **Dr. Anis ur Rahman**

Signature: _____

Committee Member3: **Dr. Muhammad Shahzad**

Signature: _____

THESIS ACCEPTANCE CERTIFICATE

Certified that final copy of MS/MPhil thesis written by Mr. **Muhammad Majid Sharif**, (Registration No NUST201464094MSEECS61314F), of MSCS-04 (SEECS) (School/College/Institute) has been vetted by undersigned, found complete in all respects as per NUST Statutes/Regulations, is free of plagiarism, errors and mistakes and is accepted as partial fulfillment for award of MS/M Phil degree. It is further certified that necessary amendments as pointed out by GEC members of the scholar have also been incorporated in the said thesis.

Signature: _____

Name of Supervisor: _____

Date: _____

Signature (HOD): _____

Date: _____

Signature (Dean/Principal): _____

Date: _____

Dedication

This Thesis is dedicated to my Mother for her love, endless support and encouragement. I would also like to dedicate my work to Father, other members of my family, Dr. Usman Akram and Dr. Asad Waqar Malik for their endless support and encouragement. Without their efforts and support, it would be a vision without action.

Certificate of Originality

I hereby declare that the research paper titled "**Extraction and Analysis of RPE later from OCT Images for Detection of Age Related Macular Degeneration**" my own work and to the best of my knowledge. It contains no materials previously published or written by another person, nor material which to a substantial extent has been accepted for the award of any degree or diploma at NUST SEECS or any other education institute, except where due acknowledgment, is made in the thesis. Any contribution made to the research by others, with whom I have worked at NUST SEECS or elsewhere, is explicitly acknowledged in the thesis.

I also declare that the intellectual content of this thesis is the product of my own work, except to the extent that assistance from others in the project's design and conception or in style, presentation and linguistic is acknowledged. I also verified the originality of contents through plagiarism software.

Author Name: Muhammad Majid Sharif

Signature: _____

Acknowledgements

I am thankful to Almighty Allah SWT, the most gracious and the most merciful. I am glad to express my sincere appreciation to my co. supervisor *Dr. Muhammad Usman Akram,* whose tremendous support and cooperation led me to this wonderful accomplishment, my supervisor Dr. Asad Waqar Malik, my committee members Dr. Anis ur Rahman and Dr. Muhammad Shahzad, for their guidance and encouragement.

Abstract

Age-related Macular Degeneration (AMD) is an eye disease which affects elderly people. Cholesterol deposits in central part of retina, known as macula, damages the photoreceptors present in a particular area of eye. AMD usually effects only central vision of patient. In medical field various imaging techniques are used for diagnosis of eye diseases. Optical Coherence Tomography (OCT) is a relatively newer technique that is found to be very useful in analyzing eyes. In this research, we used OCT images to automatically detect and classify AMD. First we extract the retinal layer known as Retinal Pigment Epithelium by utilizing Graph Theory Dynamic Programing technique, after successfully enhancing the quality of OCT image by using Wiener filter. We used a unique feature set consisting of features extracted from difference signal of RPE and Inner Segment Outer Segment layer of RPE. Feature set includes approximation coefficient, Shannon's energy, entropy and spectrum energy of the resulting difference signal. Support Vector Machine classifier was used to classify AMD affected and normal image. The developed system gives an accuracy of 95% for AMD detection.

Contents

List of Figures

List of Tables

Abbreviations

Abbreviations	Description
AMD	Age-related Macular Degeneration
CAD	Computer Aided Design
OCT	Optical Coherence Tomography
RPE	Retinal Pigment Epithelium
SD	Spectral Domain
TD	Time Domain
SS	Swept Source
SNR	Signal to Noise Ratio
KR	Kernel Regression
GTDP	Graph Theory Dynamic Programming
ISOS	Inner Segment Outer Segment
SVM	Support Vector Machine

Chapter 1

INTRODUCTION

Field of medical sciences has been using image processing techniques for decades speed up the process of diagnosis of different diseases. In medical imaging noninvasive technique used to get an image of invisible human body parts. X-Rays and MRI images two common examples of medical imaging techniques. With the emergence of computers in every field medical field also benefited from computers, with the introduction of Computer Aided Diagnostics (CAD). Use of CAD assisted doctors in diagnosing the diseases, with other benefits like better diagnosis and time saving in diagnosis process. Figure 1.1, shows some of most common techniques used in CAD systems.

Figure 1.1: MRI scan of brain (left), X-Ray of knee (Right) [1][2]

Field of ophthalmology also reaped the fruits of advancement in CAD system. CAD systems are now being used in diagnosis of retinal diseases like, Age-Related Macular Degeneration, glaucoma and diabetic retinopathy.

Age-Related Macular degeneration (AMD) is one of the retinal diseases that requires CAD system for its detection now a days. AMD usually effects the eyes of people with age above 50 years. It damages macula, a part of retina in its central part, effect in vision of a patient of AMD disease can be seen in Figure 1.2. This condition can lead to a vision loss in central part of frame. Progression time of disease differs in different persons, some people can take long time to find some abnormality, like vision loss, in others it can progress very fast. It can effect both as well one eye. AMD usually does not affect young people. AMD is spreading very fast in the world, it is expected that number of AMD affected persons from AMD will be doubled, only

in next 25 years. The main cause of AMD are drusens, these are the bright lesion deposits formed on macula. Fundus imaging has been the focus of most researchers in the past to diagnose AMD, an example of a fundus image can be seen in Figure 1.3. But we will be using OCT images a relatively newer technique for diagnosis of AMD disease.

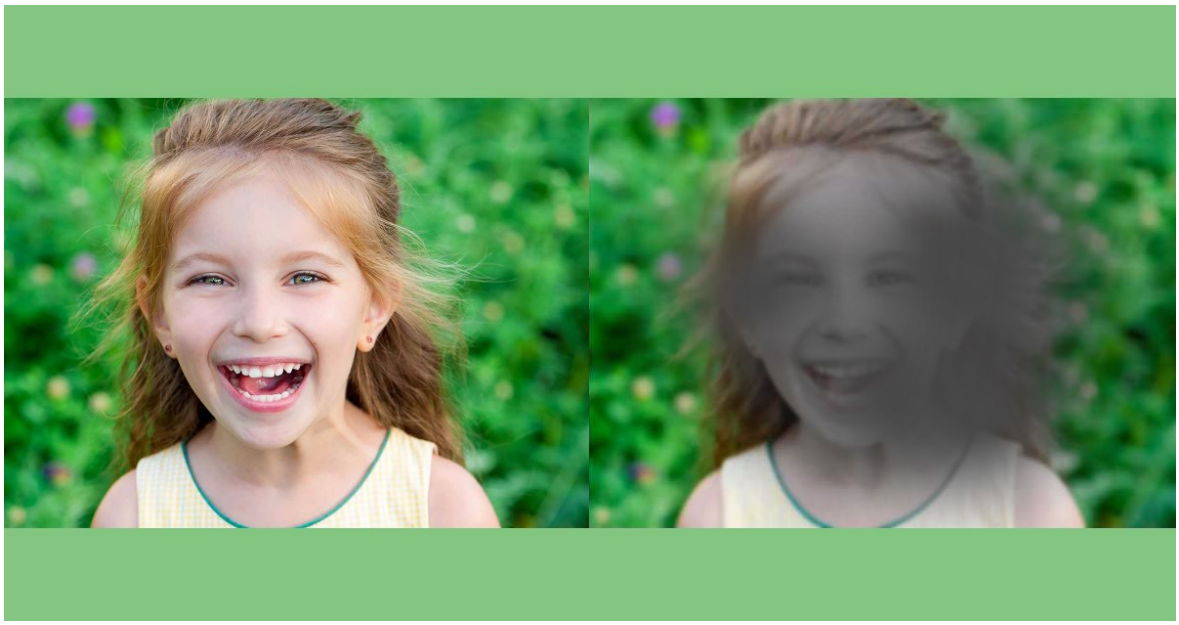

Figure 1.2: Effect of AMD on vision [3]

OCT images show cross sectional view of eye, which can be very useful in detecting AMD at early stages. Cross sectional view provided by OCT images can be a two dimensional or three dimensional image that uses the scattered light to represent this cross sectional view. Figure 1.4 shows an OCT image.

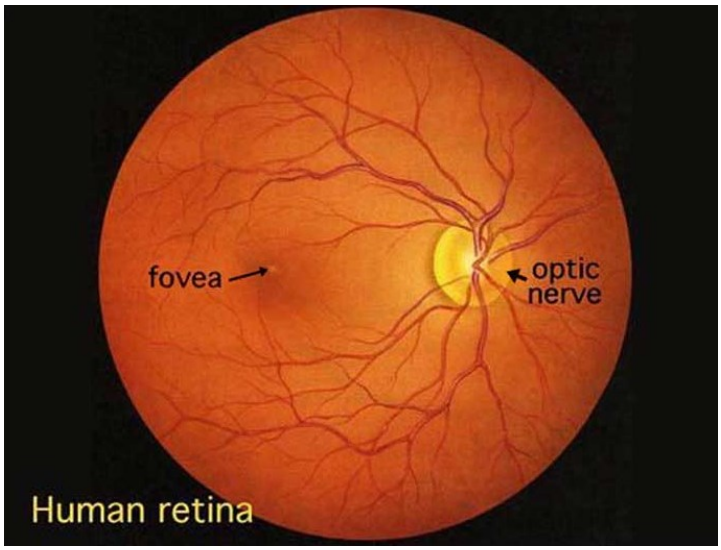

Figure 1.3: Fundus image of human eye [4]

Another advantage of using OCT image is that, the camera that takes OCT images can also be used to get fundus image so a single camera can be used to get OCT and fundus images at the same time. OCT imaging technique Use of OCT images to detect eye diseases starts way back to early 90s [5] [6]. But the technology available at that time was not very good so very limited scholars used it in their research and it also did not yield very good results because of the limitations in this technology. Main problem was the speed of acquiring the OCT images, especially in case of three dimensional OCT image, it required a large number of b-scans to form a three dimensional image. In early 2000s, with the introduction of Fourier domain optical coherence tomography in the field of ophthalmology, OCT imaging started to regain the interest of researchers. Introduction of Spectral domain OCT imaging is now a day most widely used type of OCT imaging technique. SD-OCT imaging is used because it gives high axial resolution as well as fast acquisition speed. Further details about OCT images will be discussed in Chapter 2.

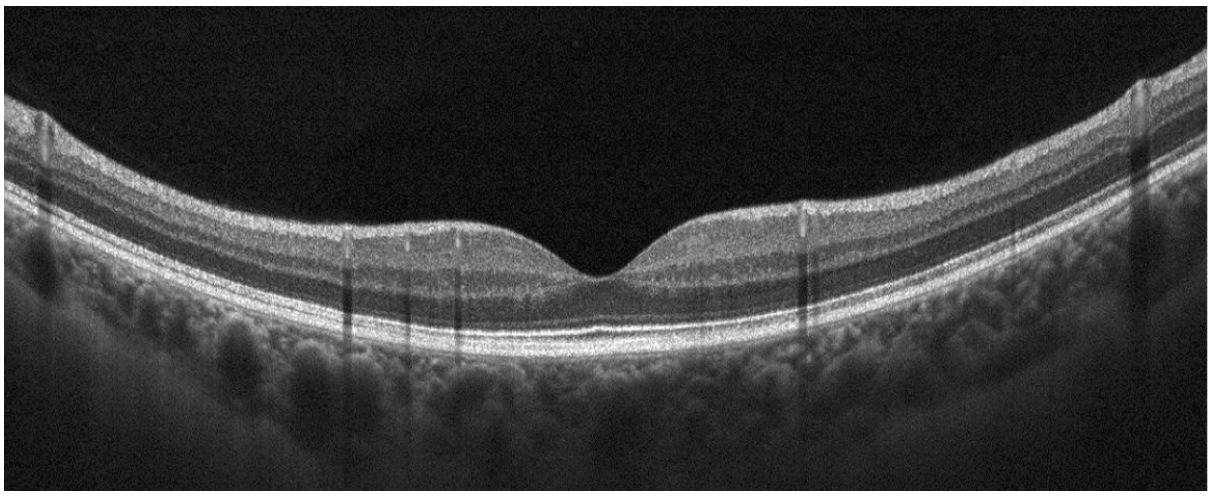

Figure 1.4: OCT image [7]

1.1 Motivation

AMD is a disease that affect retina of eye which usually leads to central vision loss, it does not affect side vision. But it can hinder daily routine of the affected person. 23.5 million people suffer from Age-Related Macular Degeneration globally [8]. Fourth most common cause of blindness after Cataracts, Preterm birth, and Glaucoma [9]. In Pakistan over 12% of population suffers from diabetes [10] which is the most common reason of AMD known as Diabetic retinopathy. Figure 1.5 depicts that Pakistan is one of the top ten countries, when it comes to number of diabetes patients, with over 6.6 million people suffering from diabetes [10]. In Pakistan because of no public policy available for diabetes, this disease has potential to rise in coming years. In Pakistan retinal OCT imaging is relatively a new field, so very less amount

of work is being done in this field. Many attempts have been made to classify AMD using different techniques but every technique had some limitations. Main motivation for this research is to find a good automated solution to detect AMD, so that further precautions can be taken to stop this disease.

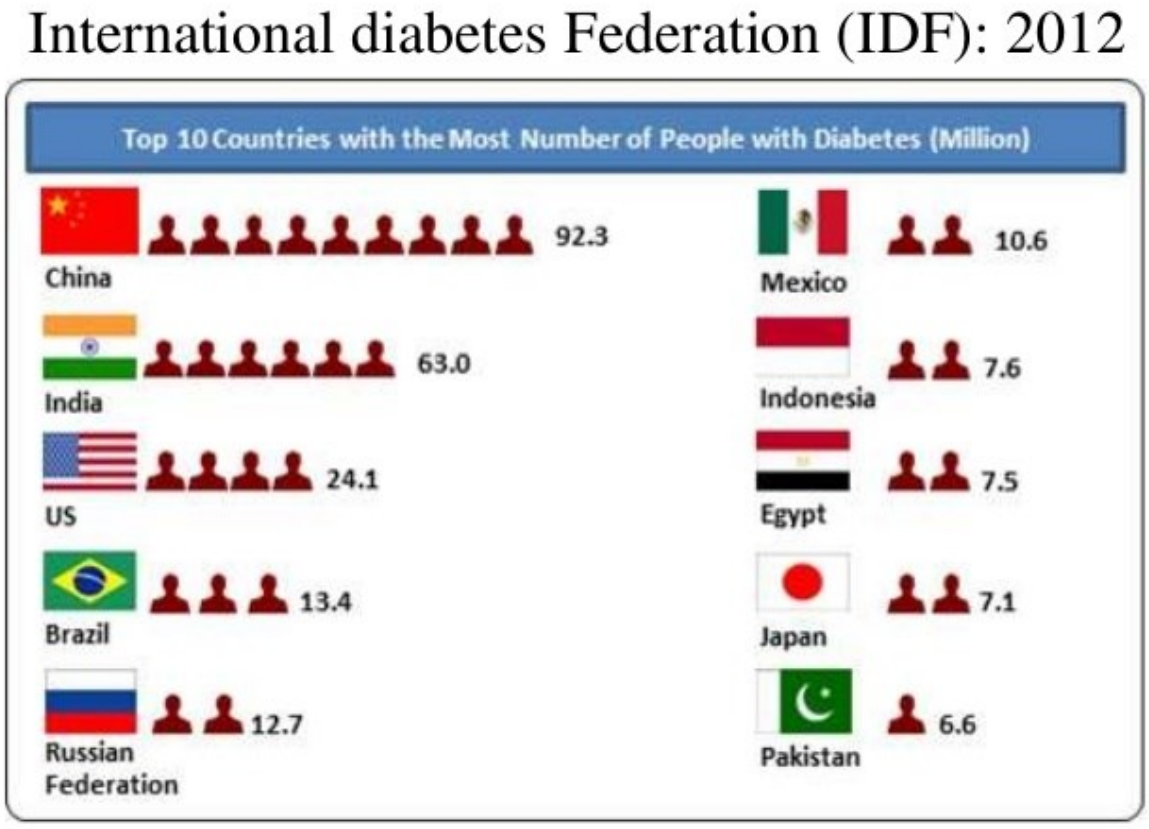

Figure 1.5: diabetes patients at risk of AMD [11]

1.2 Objectives

“ Objective of this thesis is to develop image processing algorithms along with machine learning for detection of age related macular degeneration using optical coherence tomography image. “

1.3 Challenges

OCT is relatively a newer technique so not much work is available about detection of AMD using OCT. Especially in Pakistan, very limited work is being done on detection of AMD. Some challenges faced in this work are:

1.3.1 Data Set Availability

Dataset collection was a big challenge in this project, since SD-OCT imaging is a new technique. It was difficult to find suitable dataset as equipment to get SD-OCT images is not available easily. Since Camera required for SD-OCT images is very expensive very few medical facilities have access to this camera and they too are sometimes reluctant to share their data.

1.3.2 Finding Related Work:

Another challenge was to find previous work related to AMD classification using OCT images. But being a relatively newer technique there is not too much previous work present in this field. With the coming years researchers are adopting this technique to diagnose AMD. But for now related work is very hard to find, as only a few researchers are working in this field.

1.4 Contributions

Key contributions made through this research are:

1. Retinal layer RPE was detected and extracted successfully.
2. A new technique was proposed to extract and classify AMD disease.
3. A fully automated system was developed to detect age-related macular degeneration in elderly using SD-OCT images.
4. Algorithm successfully tackles the problems faced due to bad image quality.
5. For AMD detection, 95% accuracy was achieved.

1.5 Thesis Organization

The organization of thesis is as follows:

In **Chapter 2** we discussed structure of eye, common retinal eye diseases were also discussed. In this chapter we also discuss different state of the art imaging techniques used to get images of retinal structure of eye. A detailed overview that how these imaging techniques work and are different from each other.

In **Chapter 3** we focus on state of the art techniques used for preprocessing, extraction of different retinal layers and classifying these layers. Different techniques used for Classification of drusen and retinal diseases were also discussed in this chapter.

In **Chapter 4** we explain our proposed methodology and algorithm used to find abnormality on OCT images. Complete Step by step procedure is explained to detect retinal layers and classify AMD.

In **Chapter 5** we discuss the results of the experimented algorithm.

In **Chapter 6** we conclude the thesis and discuss some future directions.

Chapter 2

2.1 Macular Eye Diseases:

The central part of retina, known as macula, is of special interest to researchers and specialists. Macula is actually a light sensitive tissue, where the light is focused coming from lens. Our ability to read and see depends on macula. It is responsible for a detailed view of structures in front of eye. Macula is often affected by diabetic retinopathy. Diabetic macular edema, which is caused by leakage of fluid in macula, is the most common cause of vision loss in young people. Another disease related to macula is age-related macular degeneration, which usually effects elderly people.

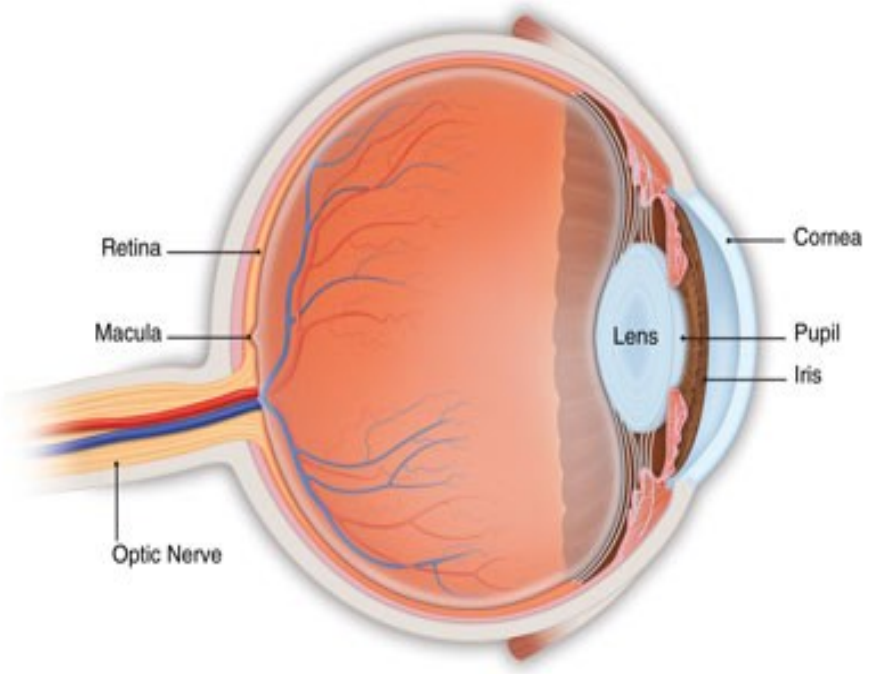

Figure 2.1: Structure of human eye

2.1.1 Age-related Macular Degeneration:

Age-related macular degeneration (AMD) is the leading cause of irreversible blindness in elderly Americans [12]. It occurs when macula, a small portion in the center of retina, depreciates. Figure 2.2 shows the effect of AMD on a healthy eye. Retina is one of the most important part of eye that consists of light sensing nerve tissue. Macula is the region in retina that is used to see the fine detail. AMD only affects central vision of eye, side vision is remains normal. Age-related macular degeneration do not cause total blindness in most of the cases. It is known as Age-related macular degeneration because it effects old age people.

Age related macular degeneration has two types.

2.1.1.1 Dry AMD:

Dry form of AMD emerges because of drusen, these are the yellow deposits present in macula. Drusen are actually tiny clumps of protein that grow in macula. Because of aging macula becomes thin and makes it easier for drusen to get in. A small drusen might not purpose changes in imaginative and prescient; but, when it grows in size, it will result in a dimming or distortion of vision that people usually discover most once they study. In later stages of dry macular degeneration, there may be also a thinning of the light sensitive layer in the macula that can lead to atrophy (also known as death of tissues). in the atrophic dry macular degeneration, affected person may have notice some blind spots located in the center of vision. Patient may lose complete central vision in later stages of dry AMD.

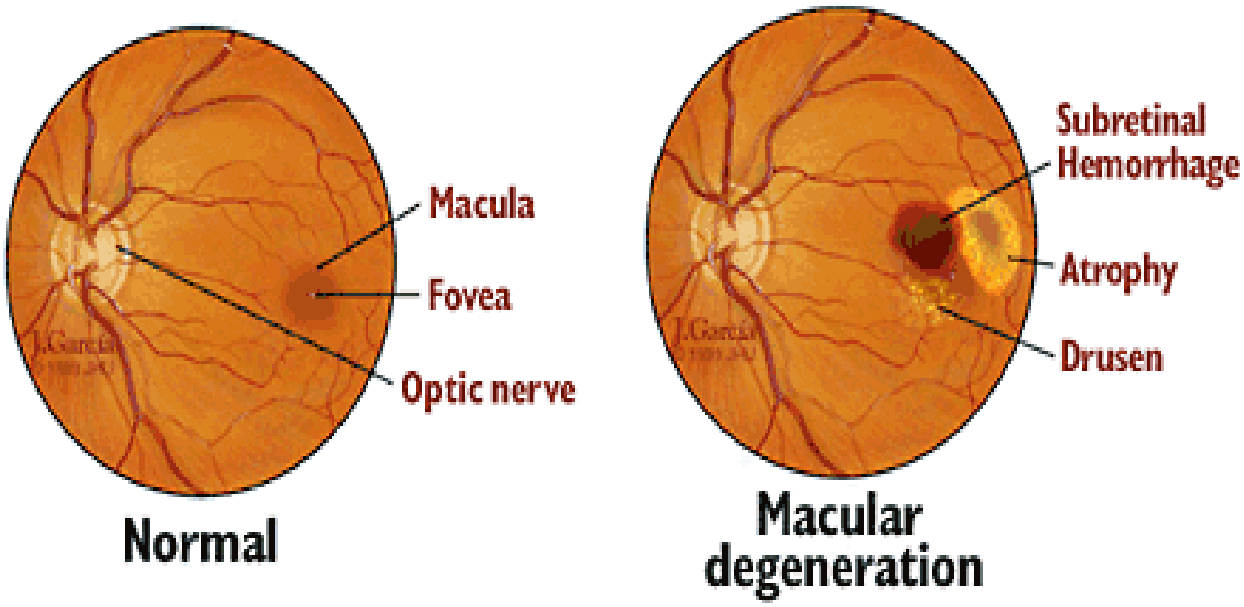

Figure 2.2: Macular Degeneration

Dry form of AMD is very difficult to treat, in fact the only treatment available is vitamin therapy. It is very important to detect this disease as early as possible, so that early vitamin therapy can be started otherwise in later stages it is very difficult or nearly impossible to treat this disease.

2.1.1.2 Wet AMD:

Wet macular degeneration occurs when blood vessels present under macula grow to an abnormal level, this phenomenon is also known as choroidal neovascularization. This condition can be seen in figure 2.3. Blood leaked in to retina from these vessels can cause some

abnormalities in vision like, straight lines can look zig zag patient can experience blind spots. Bleeding from these abnormal vessels can form a scar that can lead to the permanent loss of central vision.

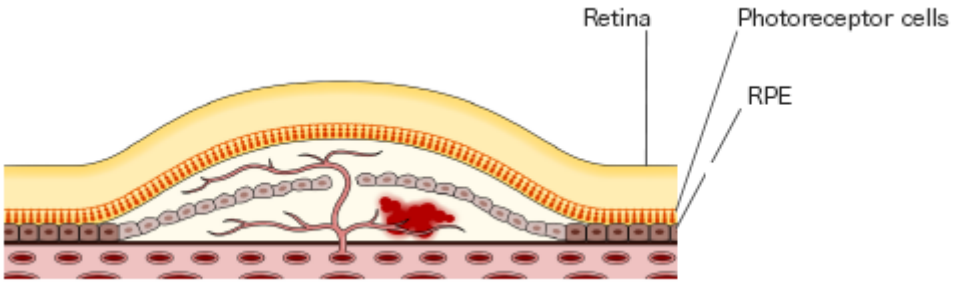

Figure 2.3: Wet AMD [13]

Dry form of AMD is more common than wet form about 90% AMD patients are diagnosed with dry AMD. However, dry AMD can eventually lead to wet macular degeneration. Though only 10% patients experience wet AMD but most of these cases suffer severe vision loss.

2.1.2 Diabetic Macular Edema:

First recognition of Macular Edema came 1856 when Jaeger published a report about diabetic maculopathy [14]. After 29 years of its discovery Nettleship confirmed these observations [14]. Macular Edema is actually accumulation of fluid in macula due to leaking of blood vessels. This results in thickening of macula, which can blur central vision and some time it can lead to central vision loss. Macular Edema effects can be seen in the figure 1.3

Figure 2.4: Vision loss because of Macular Edema [15]

2.2 Imaging Techniques Used for Diagnostics:

Macular Degeneration diseases are often diagnosed with different types of imaging techniques. These imaging techniques include.

i) Fundus Imaging

ii) Fundus Auto Florescence Imaging

iii) Optical Coherence Tomography

Fundus Imaging and Fundus Auto Florescence Imaging were used in the beginning to diagnose Macular Diseases but emergence of Optical Coherence Tomography gave a new life to the research of Macular Diseases.

2.2.1 Fundus Imaging

In Fundus Imaging or Fundus Retinal Photography a special camera is used to take pictures of internal surface of eye. Pictures are taken time to time to find any disorders present in the eye. Camera used for obtaining Fundus Images consists of a special low powered microscope attached with a camera. These cameras are labeled by the angle of view. A normal Fundus image taken by Fundus camera can be seen in image 1.5.

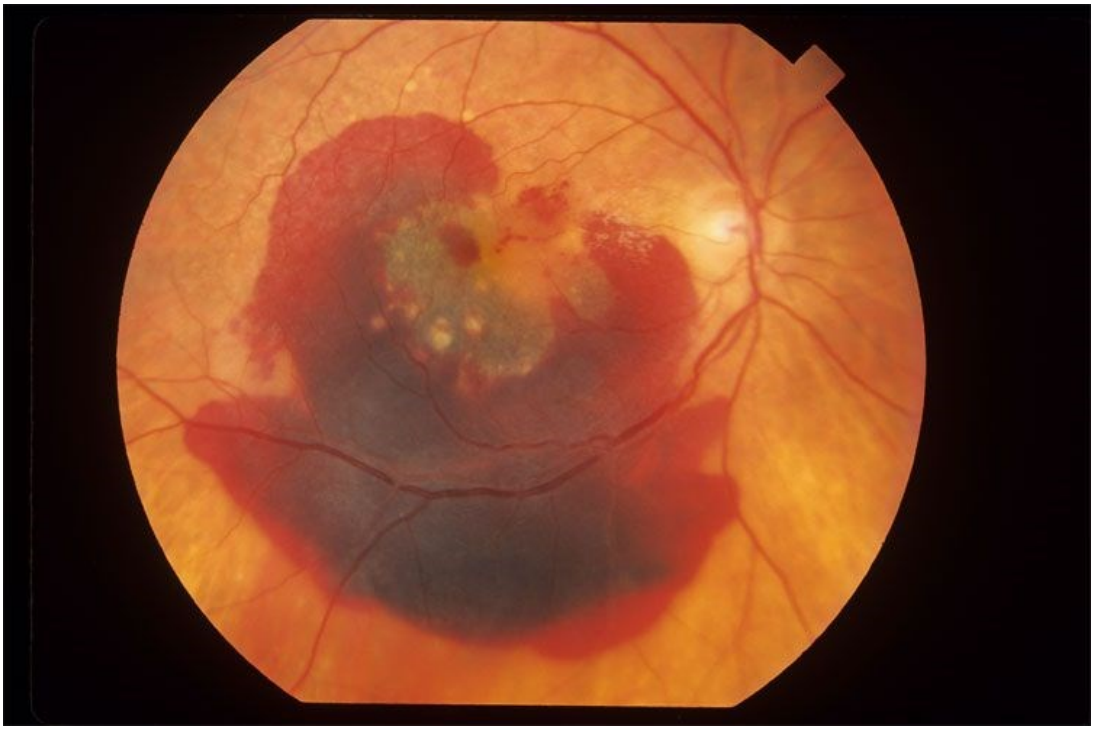

Figure 2.5: Fundus Imaging [16]

To get a normal angle of view, an angle of 30 degrees is used. It can get an image 250% larger than the real eye. To get smaller images than real eye, 45 and 140 degrees or less is used, as they give relatively less retinal magnification.

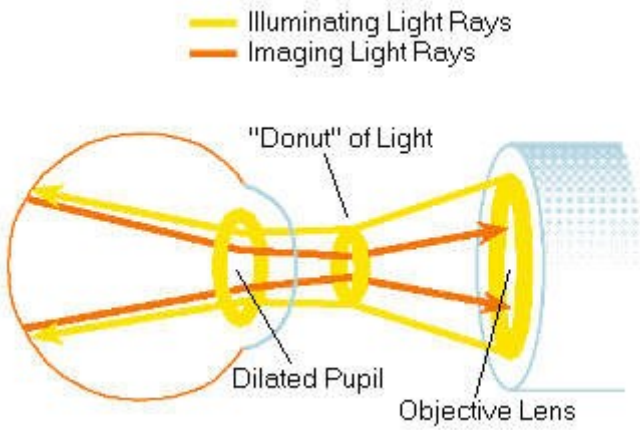

Figure 2.6: Entrance and exit of rays [17]

Fundus camera can take photograph of retina directly because for entrance and exit of illuminating and imaging rays, as can be seen in Figure 2.6. Colored filters or special filters (fluorescein and indocyanine green) can be used to perform fundus photography. A typical Fundus camera can be seen in Figure 2.7, figure also shows the internal structure of an OCT camera.

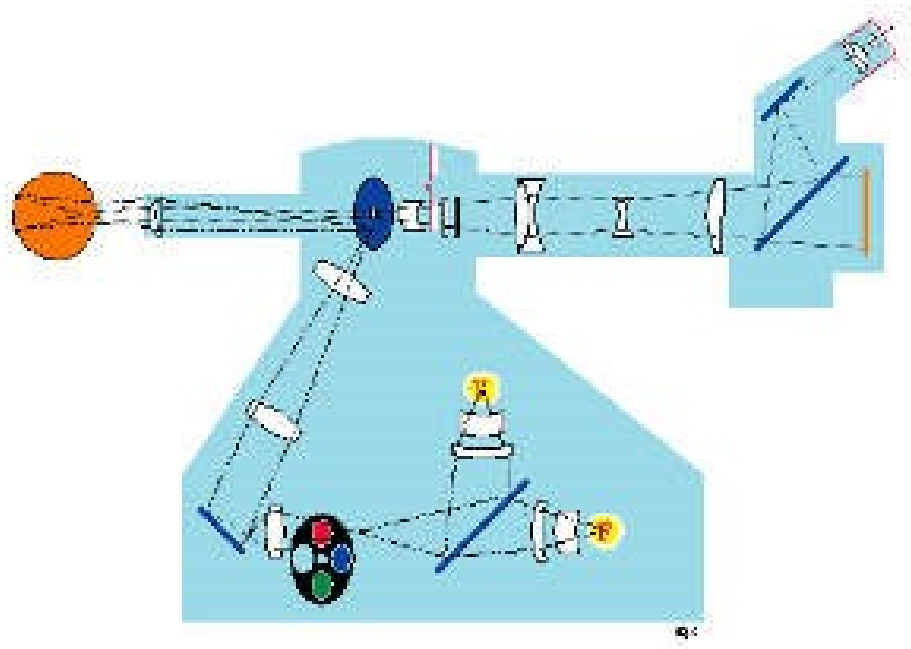

Figure 2.7: Internal structure and working of fundus camera [18]

2.2.2 Fundus Auto Florescence Imaging

Fundus auto florescence imaging is another no invasive imaging technique used to get images of AMD patients. This technique that detects fluorophores, naturally occurring molecules that absorb and emit light of specified wavelengths [19]. Auto florescence is produced by taking electrons to an excited or high energy state, it is done when photons of excitation wavelength are absorbed by a fluorophore. Some energy of electrons is used by molecular collisions, then low energy quantum of light with longer wavelength are emitted when electron is transited back to ground state. An example of auto florescence image is shown in image 2.8.

Figure 2.8: Fundus Auto Florescence Imaging [20]

2.2.3 Optical Coherence Tomography:

Optical Coherence Tomography was first determined in 1991 by Huang. et al [21]. OCT imaging was first used to show examples of weakly scattered, transparent media and high scattered, non-transparent media. In 1993 first time OCT was used to take images of Retinal Macula and optical disk [21, 22]. Initially it was only used to take cross sectional images of eyes but now it is the most widely used technique for Ophthalmology clinical applications. Figure 2.9 shows the evolution of OCT with time.

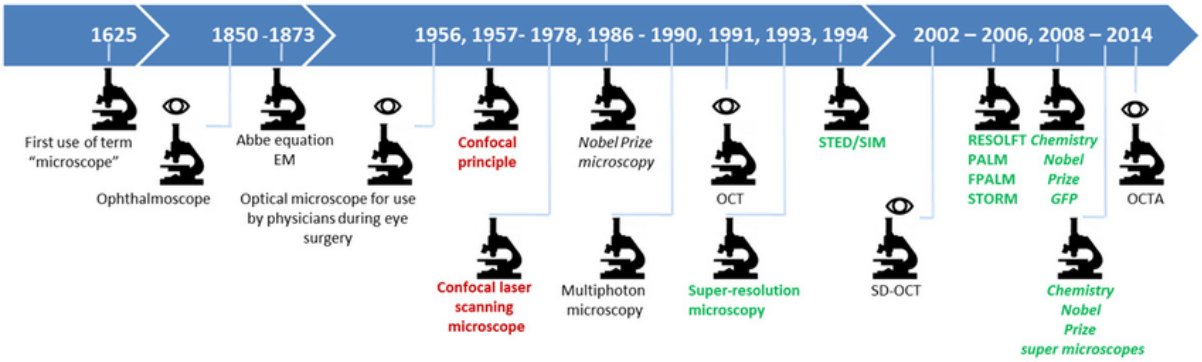

Figure 2.9: Evolution of imaging techniques [23]

Numerous variants of OCT imaging technique has emerged with time like real time high speed OCT image acquisition can take many images per second [22, 24]. Laser light source was also used to acquire high axial resolution of 1um [25].For Internal body imaging OCT imaging was acquired using endoscope and laparoscope [26, 27].

Figure 2.10: Camera used to take OCT images [28]

OCT is used to show internal structure of materials and biological system using scattered light. It provides cross sectional view of images that consists of high resolution. A common OCT camera can be seen in figure 2.10. OCT uses back reflecting through the tissues to create two dimensional or three dimensional in cross sectional plan.

2.2.3.1 Time Domain Optical Coherence Tomography:

Time domain Optical Coherence Tomography (TD-OCT) is said to be similar to ultra sound technology due to their analogous basic principles. OCT uses light source as its medium instead of sound, as in ultra sound. OCT measures intensity of reflected and back scattered light. A-Scans are created by depicting variations in optical reflectance through the depth of the tissue along a point. These single point scans are collected along the tissue to create a cross sectional view.

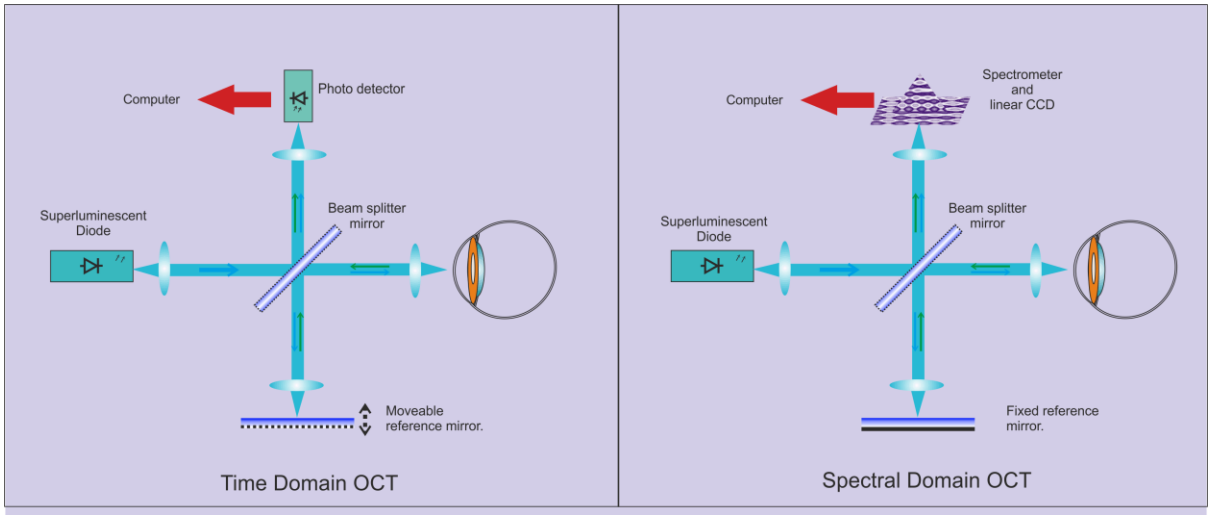

Figure 2.11: Working of OCT camera time domain (Left) spectral domain (Right)

2.2.3.2 Spectral Domain Optical Coherence Tomography:

In mid 2000s a new technique (Spectral Domain OCT) to acquire OCT images became popular, also known as fourier-domain OCT. SD-OCT greatly increased image capturing speed. SD-OCT imaging technique captures more data in less time and gives higher axial resolution, around 5um. Figure 2.11 (right) elaborates the working spectral domain OCT imaging.

Other Optical Coherence Tomography schemes currently practiced are swept-source Optical Coherence Tomography (SS-OCT), and the adaptive optics system that can be added into a SD-OCT system (AO-OCT).

Two methods are usually used to get SDOCT images. First method is spectrometer based SDOCT image, which is also known as Fourier domain OCT. This approach uses a broadband light source combined with a low loss spectrometer. It measures spectral oscillations to get final SDOCT image. Figure 2.12 and figure 2.13 further shows the internal structure of SD-OCT camera and its working in frequency domain.

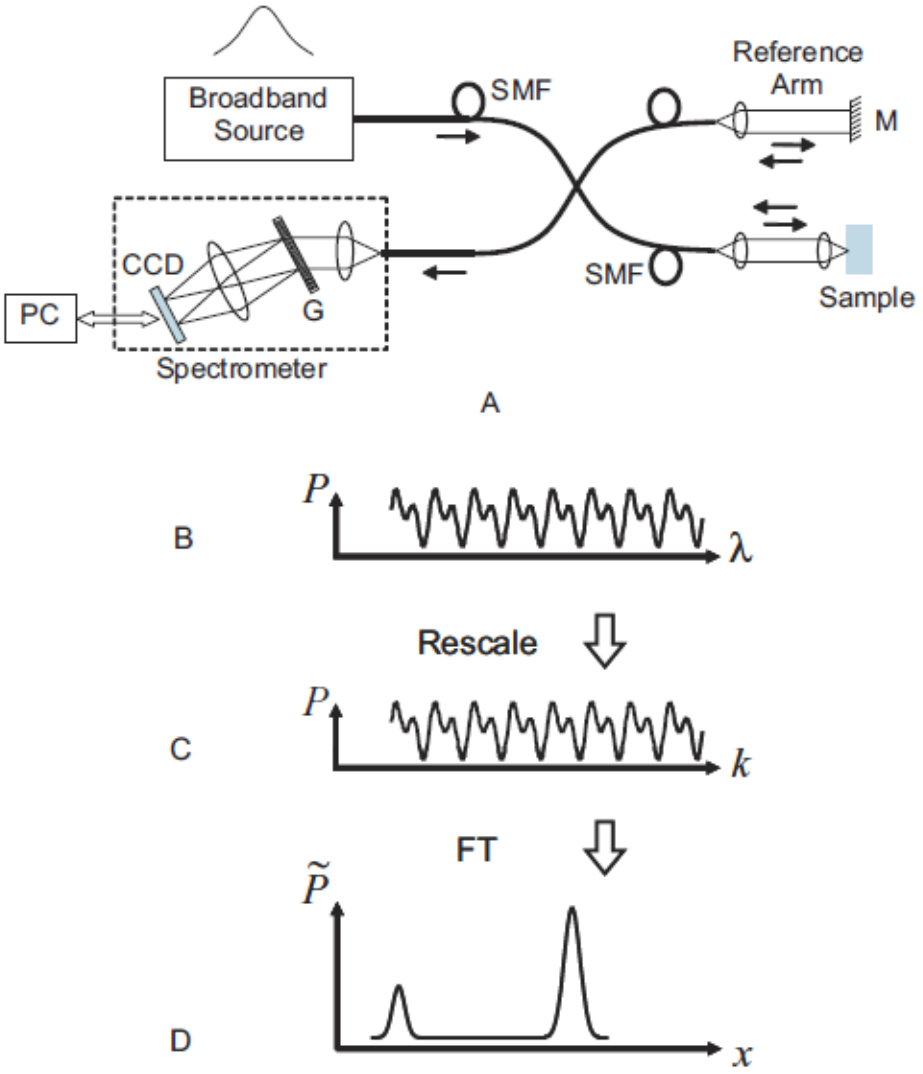

Figure 2.12: OCT camera working in frequency domain

Other approach used to get SDOCT images is swept source SDOCT, this approach is also known as optical frequency domain reflectometry (OFDR). This method uses measured spectral oscillations by employing a narrow band source at evenly spaced wavenumbers.

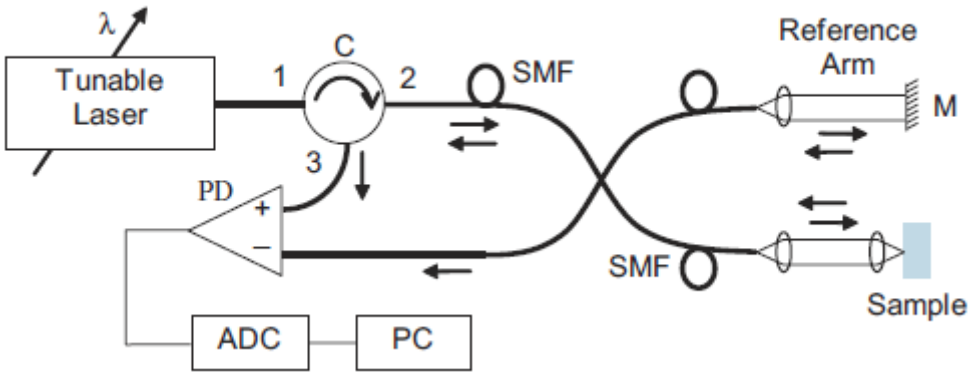

Figure 2.13: OCT camera internal structure with working principle

Chapter 3

LITERATURE REVIEW

Development of CAD system has changed the medical research field to a whole different way. Medical image processing helped the scientist to find new and easy ways to detect and diagnose different diseases very easily. Now a days completely automated system to diagnose a disease are the focus of researchers. Researchers are trying to develop new techniques to find better and speedy automated systems. In this chapter a detailed analysis about the existing techniques used for image processing will be discussed.

3.1 Pre Processing Techniques

Before we use images in our algorithm we first need to preprocess these images so that we don't need extra calculation. Preprocessing also enhances chances of better performance by the algorithm. We need to limit the processing area of image as well as the most important part of preprocessing is denoising the image. In this section we will discuss different techniques used to denoise SD-OCT images. Sparsity based denoising technique uses sparse representation dictionaries to denoise SD-OCT

images. These dictionaries are obtained by scanning some images at high signal to noise ratio (SNR) and then learn sparse representation dictionaries from these selected b-scans. Then these sparse representation dictionaries are used to denoise low SNR images. This method is known as multiscale sparsity based tomographic denoising [29].SD-OCT images acquired from OCT camera usually contain speckle noise [30]. Multi-frame weighted nuclear norm minimization method (MWNNM) is specially designed to remove speckle noise from OCT Images. This method uses weighted nuclear norm minimization [31]. MWNNM uses SD_OCT volumetric image with more than one B-scans of a small are that denoised and then average of these denoised B-scans is used to get a high signal to noise ratio B-scan [30].

3.2 Techniques Used to detect and classify Retinal Layers

First step after getting SDOCT image is to detect and classify retinal layers present in this image. Various methods have been used to find these layers. We will discuss a few methods in detail, how these methods work to find retinal layers.

KR is a non-parametric method for deriving local estimates of a function using a kernel that weighs the relative importance of nearby points [32]. While traditional KR-based applications include image denoising and interpolation [32], deblurring [33], and object detection [34].

This method uses graph theory dynamic programming to segment ILM, BM and to isolate retina. Then it uses ILM and BM segmentation to find fovea. After denoising, Kernel Regression based feature vectors are computed and then these feature vectors are used to classify retinal layers. Only selected features and weights were used for classification using a special method known as wSFFS, then tenfold cross validation was used to get desired results. Deformable models is one of the vigorously researched techniques in image processing field. This technique combines approximation theory, physics and geometry. Deformable models are very useful in segmenting and extracting structures from images using size shape and structure of images. G Tsechpenakis et al proposed a geometric model based on CRF that was capable of automatically detecting geographic atrophy present in AMD effected eyes [35]. SD-OCT images were used to get internal structure of macula.

Macular thickness parameters are also used to identify unhealthy eyes using OCT images. A normative database, where thickness measurements of healthy macula are saved, is generated by taking OCT images of identified normal persons, as well as patients with macular disease, as a training set. Then this dataset is used to compare thickness parameters of a new test case. F. A. Medeiros et al also used thickness measurement as their primary method to find the relation between unhealthy and normal eyes. F. A. Medeiros et al presented a method in which they use thickness parameters and retinal nerve fiber layer to find the difference between healthy and effected subjects [36]. Another method used the axial distance from Bruch's membrane and the RPE also the distance between Bruch's membrane and the inner limiting [37]. These thickness measurements were then used to find an averaged thickness map and then these maps were used to form an automated classifier to find the relation between healthy and effected macula. Another model presented by G. Gregori et al used thickness measurement methods to find area of the drusen. Author used manual method to detect macula. According to their findings G Gregori et al found that early AMD consisted of less than 63μm area of drusen, intermediate AMD consisted of 63μm to 125μm area of drusen whereas advanced AMD with large drusen was found to be more than 125μm [38]. Some researchers used texture and morphological features to detect abnormality in retinal layer and macula. One of the methods used by R. Koprowski et al used morphological features and texture to find drusen present in macula [39]. They used OCT images to find the presence of AMD in subject. Detection of neovascular AMD using morphological and texture features was 73 percent accurate. Authors also found ischemia present in inner layers of retina with an accuracy of 83 percent and fibrovascular tissue scaring with 69 percent accuracy [39]. Another recent approach used by Y. Zhang et al is kernel principle components model. Accuracy rate to

differentiate between AMD affected eyes and normal eyes achieved was 92% [40]. Y. Zhang et al used 3D OCT retinal images dataset. P. P. Srivnvasan et al used histogram oriented gradient to detect eye diseases related to retina. Table 3.1 provides a summarized review of different techniques used by researcher so far.

RF Spaide used genetic risk alleles to predict the future course of AMD [41]. He also proposed that most models designed to detect AMD because they did not cover pseudo drusen, neo vascularization subtypes and polypoidal choroidal vasculopathy [41]. In another recent study Cecilia S. Lee et al implemented a system that used deep learning neural networks to classify between AMD and normal images. They achieved an accuracy of 87.63%.

TABLE I: Summary of Existing Systems and Techniques

Authors	**Purpose**	**Method**	**Performance**
Leyuan Fang [29]	Noise Removal	Sparsity Based Denoising	-
Damber Thapa [30] 2015	Noise Removal	Multi-frame Weighted Nuclear Norm Minimization	-
G Tsechpenakis [35]	Detecting geographic atrophy and AMD clasification	Deformable models	97% accuracy
S. Zhang [31]	AMD clasification	Weighted Nuclear Norm Minimization	82% accuracy
F. A. Medeiros [36]	AMD clasification	thickness parameters and retinal nerve fiber layer	-
S. Farsiu [37]	AMD clasification	axial distance from Bruch's membrane and the RPE	-
G. Gregori [38]	AMD clasification		-
R. Koprowski [39]	AMD clasification	Texture and Morphological features	73% accuracy
Y. Zhang [40]	AMD clasification	kernel principle components model	92% accuracy
P. P. Srinivasan [42]	AMD clasification	histogram of oriented gradient	95% accuracy
Cecilia S. Lee	AMD clasification	deep learning neural networks	88% accuracy
RF Spaide	AMD clasification	genetic risk alleles	-

CHAPTER 4

METHODOLOGY

Purpose of this thesis is to build a system that takes a SD-OCT image, find retinal boundaries and then classify it into a AMD effected or normal image. Complete process is shown in figure 4.1.

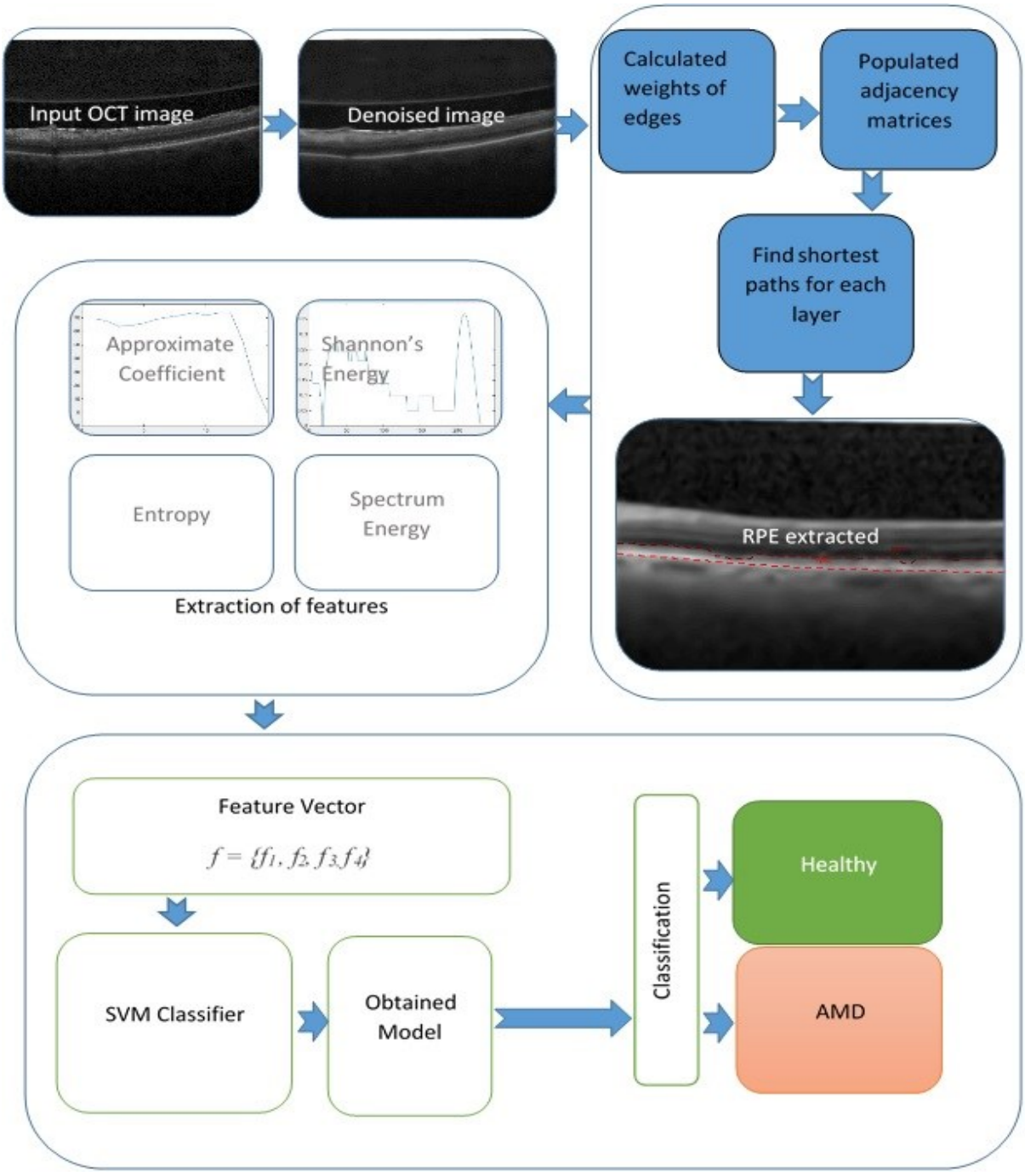

Figure 4.1: Methodology flow diagram.

4.1 SD-OCT Image

As input we take an SD-OCT image from user. This SD-OCT image is taken by a special camera used for these images. OCT images focuses on retina of the subject's eye. Collected OCT image can be seen in figure 4.1.

4.2 Denoising Image

OCT images collected contained speckle noise. Because of speckle noise detection process of layers from OCT image can be effected.

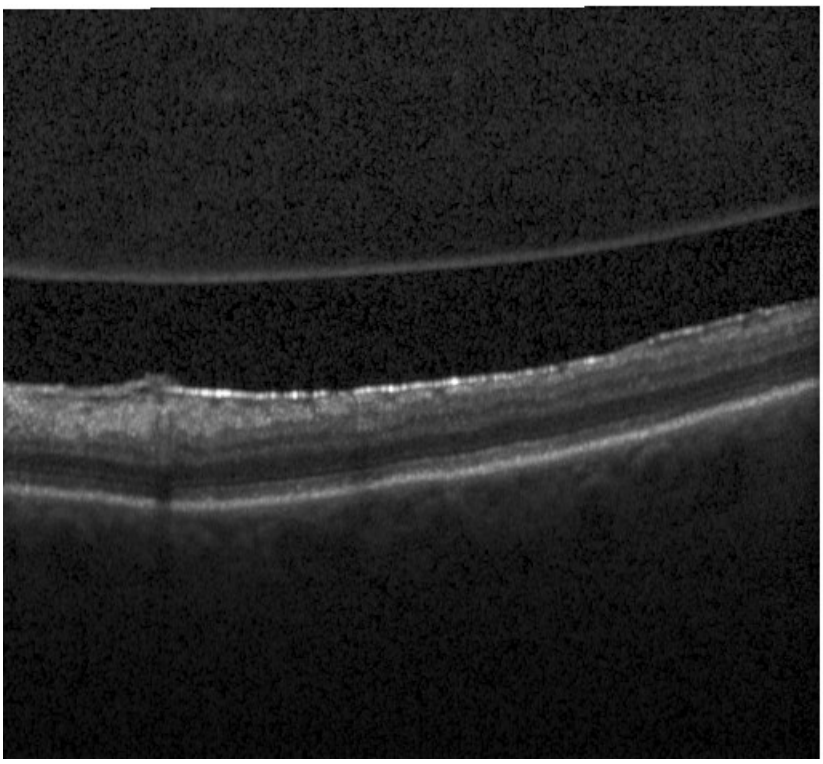

Figure 4.2: input OCT image.

This image cannot be used to implement graph theory Dynamic Programming algorithm, because speckle noise can downgrade the results obtained from GTDP.

Our first priority was to remove the noise but keep the shape of macular layers intact. For removing speckle noise, we used Weiner Filter. Same image as in figure 4.2, when passed through Weiner filter to remove noise can be seen in figure 4.3.

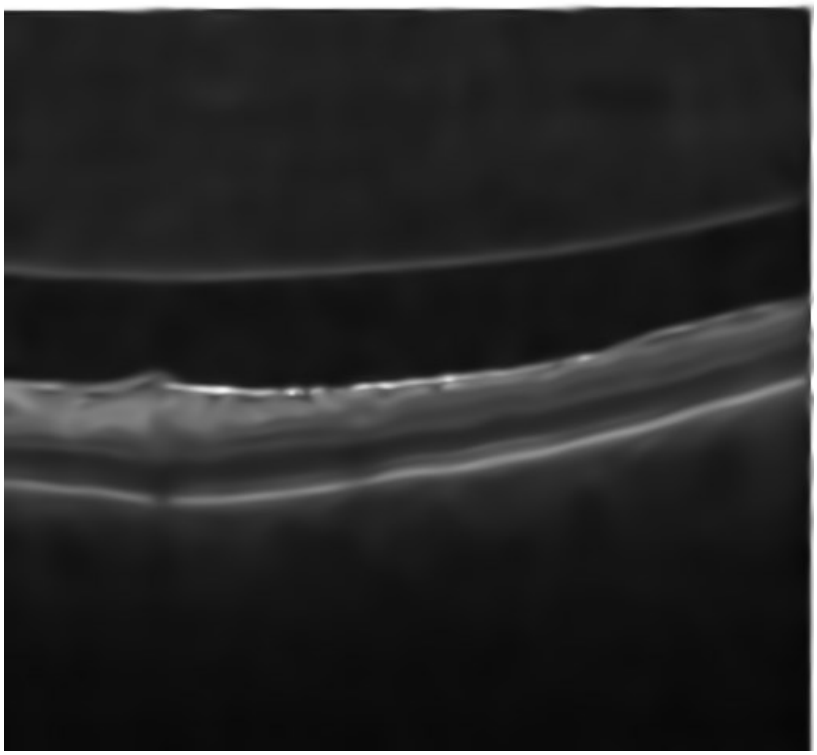

Figure 4.3: Denoised image.

4.2.1 Weiner Filter

Weiner filter uses liner time invariant filtering to denoise a noisy image. An estimated new image is produced by using statistical estimate of the image.

4.3 Extractions of RPE and ISOS

To find RPE from a denoised OCT image, Graph Theory Dynamic Programming was used. Given image is a set of pixels and we can represent each pixel as a node of a graph, so we represent the image as a graph of nodes. These nodes are connected by edges. We can also assign weight to each edge to maintain connectivity across the graph.

First of all two extra columns are added with the highest edge weight to initialize the process from left top corner, see Figure 4.4.

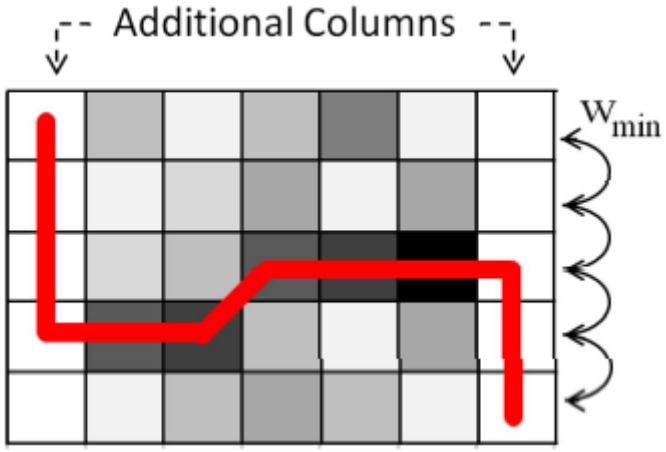

Figure 4.4: Finding minimum weighted path.

Edges are assigned weight according to their respective pixel intensity.

4.3.1 Limitation of search region

Sometimes, layer that needs segmentation can have similar features as of some other structures in the neighborhood. So we need to get rid of these analogues structures first so that we may not accidently segment a wrong layer. For that purpose we use the technique of limiting the search region, in which we remove the weights of the regions we do not need. When we successfully find a layer we declare all the nodes and region that is present above it as invalid region by removing its weights from graph.

4.3.2 Extraction of Minimum weighted path

Once we determine the start and the end point we can use any path finding algorithm. We used Dijkstra's Algorithm to find the path with the minimum weight in graph. Figure 4.4 elaborates the process of extraction of minimum weighted path from a given gray scale image.

4.3.3 Segmentation of ISOS/RPE

ISOS/RPE is the brightest and the most prominent layer in OCT image. But vitreous-NFL is also very prominent. These layers consist of high contrast in SD-OCT image. So when we use Dijkstra's algorithm the resulting cut do not make it clear that if it's vitreous-NFL or ISOS/RPE.

To discriminate between vitreous-NFL and ISOS/RPE, we first find if hyper reflectivity is present or not in this region. Because vitreous-NFL contains some hyper reflectivity exactly above it because it is the top most layer in the B-scan. So if we find hyper reflectivity than we can say it's vitreous-NFL, otherwise RPE.

To find hyper reflectivity we pass this image through a low-pass filter and to get required low-pass we use Gaussian Kernel. Then we use Otsu's method to generate a binary mask for thresholding. Then we calculate the fraction for bright pixels present in the above region. This fraction is then analyzed if it's more than 0.025 than the layer is classified as vitreous-NFL otherwise as ISOS/RPE.

4.4 Finding Difference and Shannon's Energy

Once RPE was extracted from image next step was to find its Shannon's Energy (SE). To find SE of subject image we first find the difference between RPE and ISOS, as we can see from the given formula. Graph obtained from f[n] can be seen in figure 4.4.

$$f[n] = rpe[n] - isos[n]$$

After finding f[n] we used following formula to find Shannon's Energy.

$$\mathrm{SE} = -|a[n]| \log(|a[n]|),$$

$$s[n] = -a^2[n] \log\left(a^2[n]\right),$$

Figure 4.5 shows the Shannon's energy signal of given image.

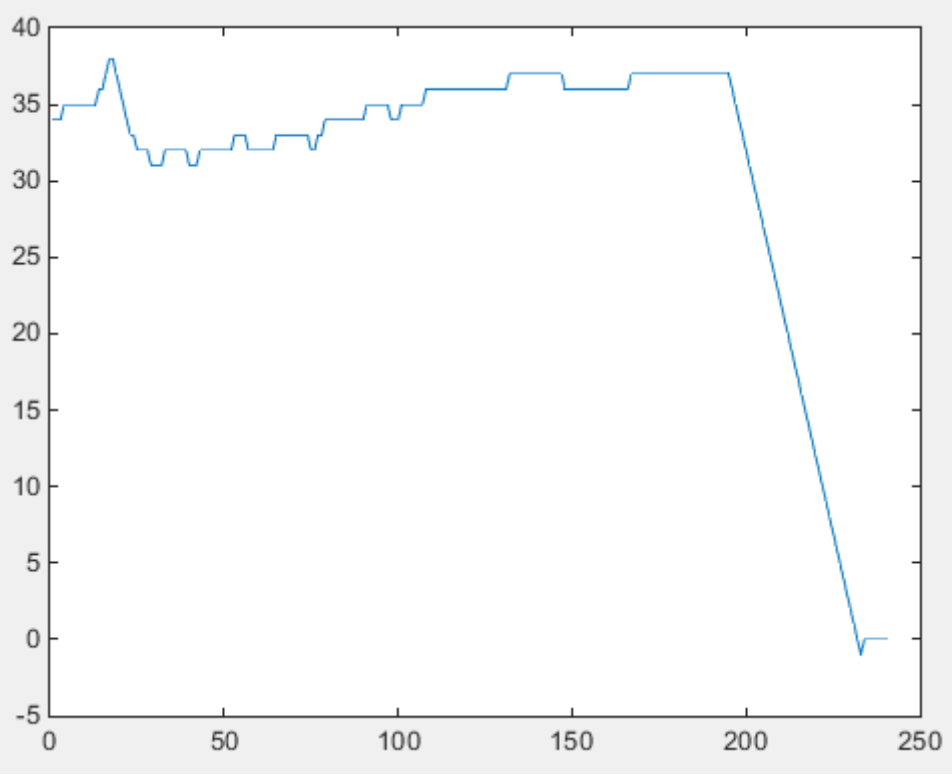

Figure 4.5: Difference between RPE(ISOS) and RPE(interpolated)

Where a[n] is the normalized difference of RPE and ISOS and its formula is given below.

$$a[n] = \frac{|f[n]|}{\max_{i=1}^{N} |f[n]|},$$

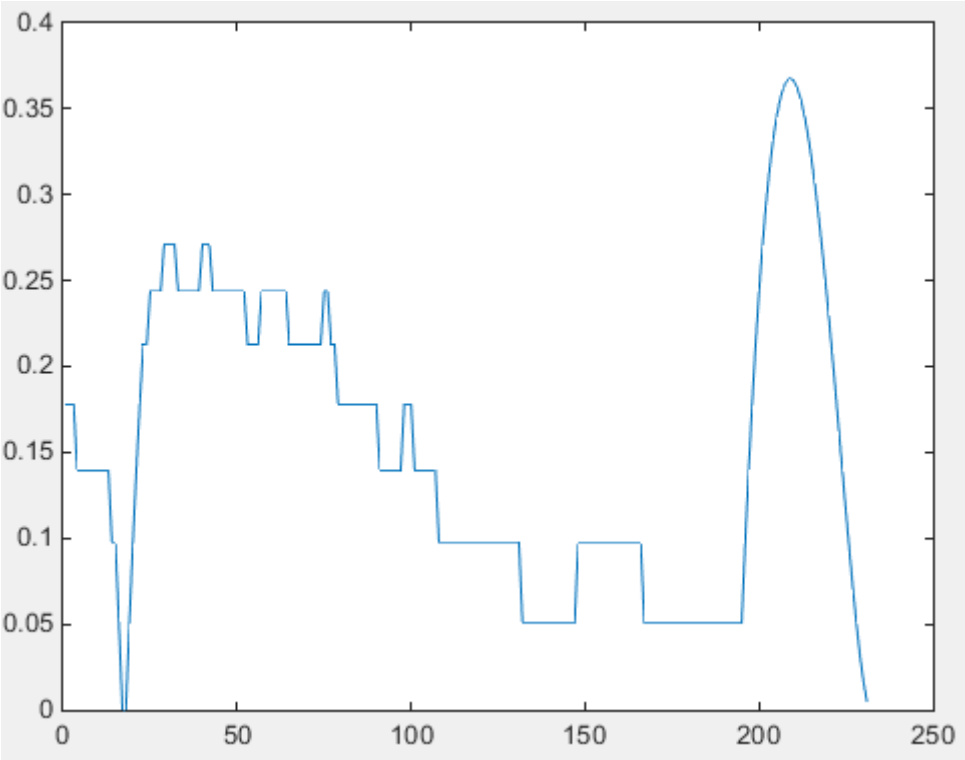

Figure 4.6: Shannon's energy of difference signal

4.5 Decomposition of Signal

For further analysis resulting signal is decomposed. In the first step decomposed wave gives two coefficients, known as approximation coefficient (A1), can be seen in figure 4.6 and detail coefficient (D1), can be seen in figure 4.7. To get approximation coefficients given signal is convolved with a low pass filter. Similarly for detail coefficient high pass filter is used for convolution.

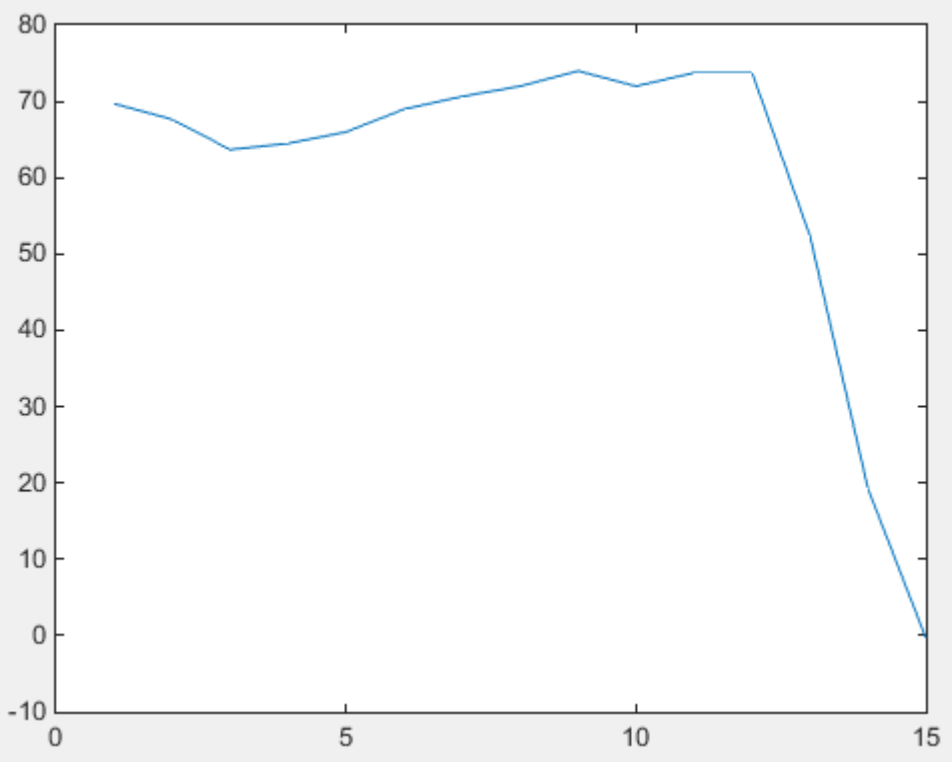

Figure 4.7: Approximation coefficient of decomposed signal

Each filter is of length 2n and the length of each coefficient can be calculated by using following formula

$$\text{floor}\left(\frac{n-1}{2}\right)+N$$

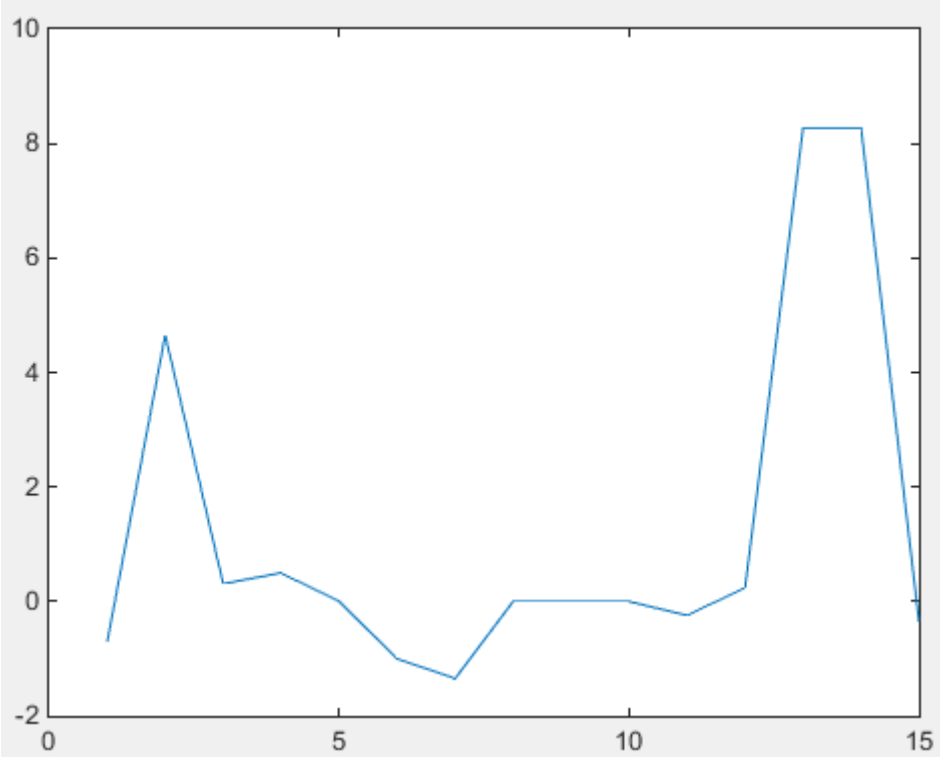

Figure 4.8: Detail coefficient of decomposed signal

When we decompose the signal obtained after finding SE it forms a tree like structure as we can see in figure 4.8. We use decomposition of wavelet only up to two levels.

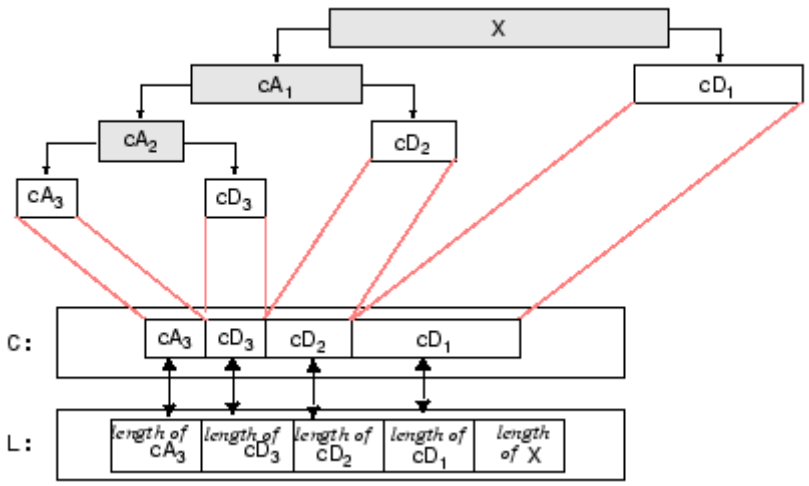

Figure 4.9: Decomposition of signal

4.6 Maximum Value of A1

As we only decomposed the wavelet up to level two we are only concerned with level of decomposition we find the maximum value of approximation coefficient A1. Maximum value of coefficient will be used as a feature in SVM training.

4.7 Entropy

Based on Shannon's information theory Spectral Entropy actually measures index of complexity from an uncertain system. Entropy measures the change in nonlinear dynamic states without too much of data overhead. Values calculated by spectral entropy can be used a feature for training purpose in SVM training.

For an uncertain system where random variable is X with the values,

$$X = \{x_1, x_2, \cdots, x_n\} \qquad (n \geq 1)$$

Equivalent probability can be found as,

$$P = \{p_1, p_2, \cdots, p_n\} \; 0 \leq p_i \leq 1, i = 1,2, \cdots, n$$

Where,

$$\sum_{i=1}^{n} p_i = 1$$

Once we know all the requiremnets, we calculated entropy of the signal by using the following formulla.

$$H = -\sum_{i=1}^{n} p_i \ln p_i$$

4.8 Spectrum Energy:

It is not possible to find frequency components of a signal by looking at its shape, so we need to take this signal in frequency domain. Fast Fourier Transform is one way to do that.

Energy Spectral Density is a measure of variations in the strength of a signal or energy by using a function of frequency. This function shows at which frequencies, energy of the signal is strong and at which point it is weak.

Since we know that RPE is the brightest layer in an OCT image of macula. So we used it's flux density to find spectral energy.

For signal x(t) energy of the signal E can be calculated by using the following formula.

$$E = \int_{-\infty}^{\infty} |x(t)|^2 \, dt.$$

An alternate formula to calculate energy is.

$$\int_{-\infty}^{\infty} |x(t)|^2 \, dt = \int_{-\infty}^{\infty} |\hat{x}(f)|^2 \, df,$$

Where

$$\hat{x}(f) = \int_{-\infty}^{\infty} e^{-2\pi i f t} x(t) \, dt,$$

Is known as Fourier Transform of the signal and the integral on the right hand side is the actual energy of the signal.

4.9 Forming a feature vector:

After collecting all the required features, we compile a feature vector that will be used in classification of AMD. Table II shows feature values extracted from random images

TABLE II: Sample values of features

Type	Case	Features		
		F1	**F2**	**F3**
Healthy	Case 1	92.2931034482759	3.58989809546429	8.77780701680490
	Case 2	95.5000000000000	3.37355726227519	8.68206545857989
	Case 3	96.3793103448276	3.45656476213095	8.65475966894741
	Case 4	94.3620689655173	3.45656476213095	8.63239687687579
	Case 5	94.2068965517242	3.37355726227519	6.71629255355159
AMD	Case 1	85.5000000000000	3.64022392894185	10.5185367197630
	Case 2	83.1896551724138	3.90689059560852	9.84659797578458
	Case 3	86.5000000000000	3.45656476213095	10.1200852719649
	Case 4	89.0000000000000	3.77355726227518	9.85710924211307
	Case 5	88.7758620689655	3.50689059560852	10.3125917257990

4.10 Classification using SVM:

Support Vector Machine is used to classify the images. Feature vector obtained from difference signal is given to SVM. Training dataset is provided to SM to create a model. This model is then used to classify any input image given the system as a testing image.

Chapter 5

RESULTS

5.1 Dataset

In Pakistan, no big enough dataset of OCT images is present that can be used for such system to train the parameters. So we acquired a custom dataset from Duke University. Vision and image processing laboratory at department of ophthalmology, Duke University provided a dataset that consisted of 1020 b-scans of total 269 AMD patients and 115 normal subjects. This dataset consists of SD-OCT images consisting of B-scans from subjects. This dataset is open source, so that anyone can use it, on Duke University website [43].

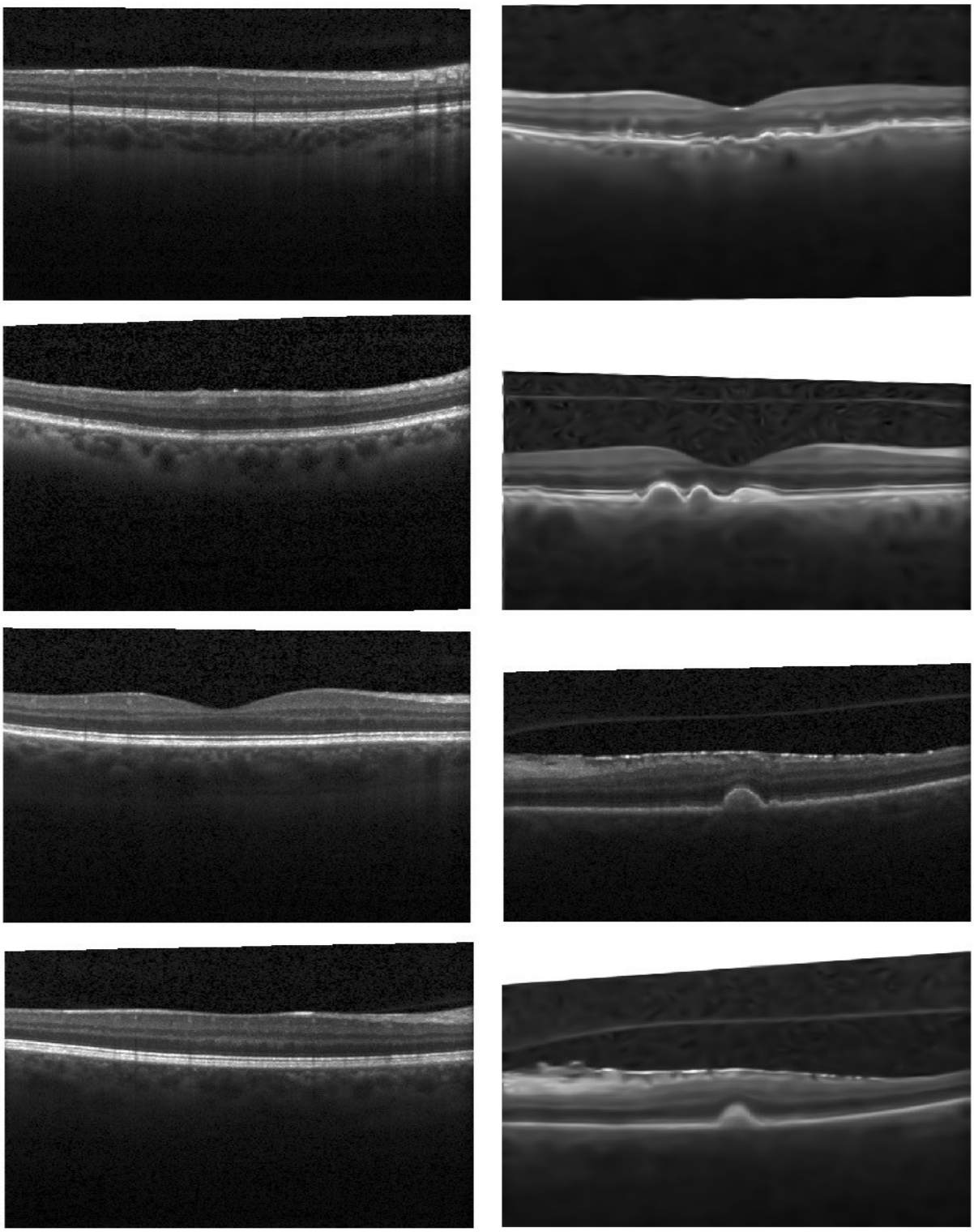

Figure 5.1: Sample input dataset, Normal subject (left), AMD subject (right)

5.2 Results

The performance of the proposed system is measured by running this algorithm on test images. These images are part of our dataset, detail of our dataset is given in section 5.2. A total of 950

images were used for training and testing purpose. Out of these 950 images 446 images contained AMD disease and remaining 504 images were of healthy macula. Out of 446 images 424 images (with AMD) were correctly classified. Similarly out of 504 images with normal 469 were correctly classified by our algorithm. Figure 5.1 shows a sample dataset. Left side images in figure 5.2 show OCT images of normal subjects and right side of the image shows OCT images of subjects suffering from AMD.

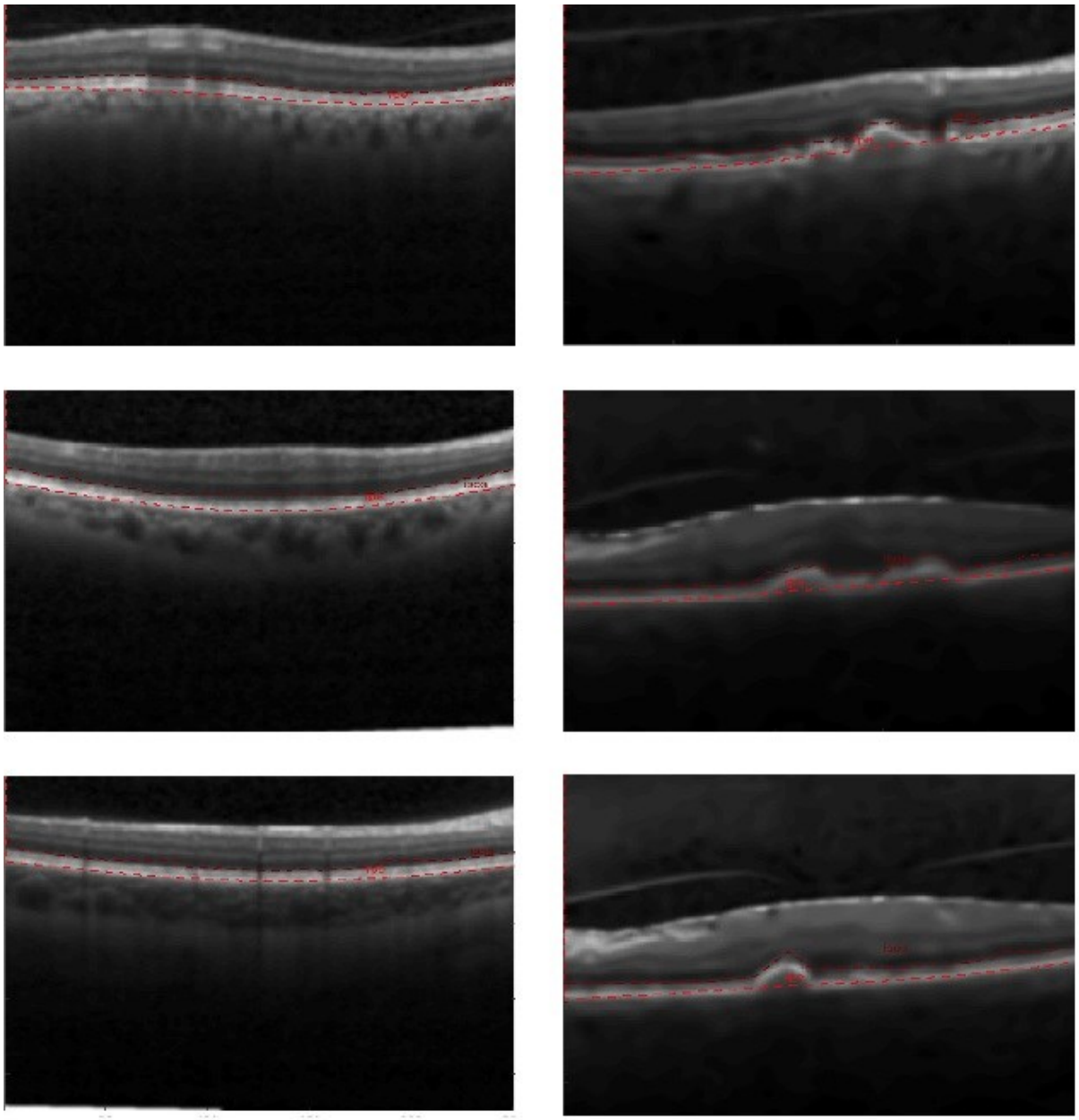

Figure 5.1: RPE extraction from input OCT images

In figure 5.1 extracted RPE from given images after all the processing is shown. Upper dotted line in maroon color shows the outer boundary of RPE, whereas lower dotted line in red color shows the expected placement of original RPE.

TABLE III: Results

Type	No. of images	Correctly classified	Incorrectly classified
Normal	504	469	35
AMD	446	424	22
Total	950	893	57

Table III illustrates the overall results of the implemented algorithm. Table IV describes mean and standard deviation for different features used to classify AMD disease.

TABLE IV: Feature Characteristics

Subject	Value Type	F1	F2	F3
Normal	Mean	94.4389	3.5570	8.6117
	Std. Deviation	14.3705	0.1884	1.0093
AMD	Mean	87.7447	3.6816	10.1546
	Std. Deviation	20.7536	0.1683	1.4675

Results collected from proposed algorithm shows that we achieved 93% accuracy, 95% sensitivity and 93% specificity, see Table V.

TABLE V: Algorithm Performance

Type	Correctly Classified	Accuracy	Sensitivity	Specificity
Healthy	469/504	94%		93%
AMD	424/446		95%	

Sensitivity means true positive rate or number of AMD victims that are correctly identified as AMD positive in our case.

Specificity means true negative rate or number of healthy subjects that were classified as healthy by our algorithm.

Accuracy means overall performance of a system or total number of correctly classified subjects.

Chapter 6

CONCLUSION AND FUTURE WORK

6.1 Conclusion

In recent years biomedical image analysis and processing techniques are gaining popularity. Different image processing techniques are capturing interest of researchers working in biomedical field. Automated diagnosis of different diseases using different image processing techniques has helped physicians in early detection of diseases in more reliable manner, so that early treatment of diseases can be started. AMD is an eye disease that can damage central part of eye called macula. If this disease is no detected at early stage it can lead to permanent central vision loss. Early stage of AMD also known as dry AMD is usually found in elderly population. If not cured early it can lead to a more sever case known as wet AMD, that is responsible for permanent vision loss.

In this thesis we proposed and developed a system to detect and classify AMD that is fully automated. The system uses OCT images as input. Selection of OCT imaging was made because it is comparatively a new technique and it was found that it is easy to classify AMD disease using OCT images. Implemented system was able to classify most of the images accurately. Proposed system was found reliable while diagnosing the disease. Actual aim of the system was to diagnose AMD disease in earlier stages. Preprocessing was done to enhance the quality of images. For RPE detection graph theory dynamic programming was used. Then images were classified with the help of support vector machine. Results collected from the test dataset were very encouraging overall accuracy of 94% was achieved.

6.2 Future work

Based on this research, in future, this algorithm can be used to detect other diseases like glaucoma and other eye diseases. This algorithm can also be useful to automatically detect and classify brain tumors and other brain diseases. This research focuses on use of 2D images, this research can be further enhanced to use 3D OCT images.

References

1. MRI scan of brain [online] Available at: http://www.valleyradiologync.com/sites/default/files/brain-scan-MRI-500x282.png
2. X-Ray of knee [online] Available at: https://www.mayoclinic.org/-/media/kcms/gbs/patient-consumer/images/2013/11/15/17/37/my00307_-my00710_im04134_mcdc7_kneearthritisthu_jpg.jpg
3. Age-related Macular Degeneration [online] Available at: http://i1.allaboutvision.com/i/conditions-2016/amd-little-girl-1200x630.jpg
4. Fundus Image [Online] Available at: http://webvision.org.es/gross-anatomy-of-the-eye/1-2-simple-anatomy-of-the-retina/
5. Fercher AF, Mengedoht K, Werner W, "Eye-length measurement by interferometry with partially coherent light." Opt Lett. 1988 Mar 1; 13(3):186-8.
6. Swanson EA, Izatt JA, Hee MR, Huang D, Lin CP, Schuman JS, Puliafito CA, Fujimoto JG, "In vivo retinal imaging by optical coherence tomography." Opt Lett. 1993 Nov 1; 18(21):1864-6.
7. OCT image of normal eye [Online] Available at: https://www.clinicabelfort.com.br/wp-content/uploads/2016/03/oct-normal-clinica-belfort.jpg
8. Velez-Montoya, R; Oliver, SC; Olson, JL; Fine, SL; Quiroz-Mercado, H; Mandava, N (March 2014). "Current knowledge and trends in age-related macular degeneration: genetics, epidemiology, and prevention.". Retina (Philadelphia, Pa.). 34 (3): 423–41.
9. Global Burden of Disease Study 2013, Collaborators (22 August 2015). "Global, regional, and national incidence, prevalence, and years lived with disability for 301 acute and chronic diseases and injuries in 188 countries, 1990–2013: a systematic analysis for the Global Burden of Disease Study 2013." *Lancet (London, England)*. 386 (9995): 743–800.
10. www.who.int/diabetes/country-profiles/pak_en.pdf
11. Image [Online] Available at: https://image.slidesharecdn.com/diabetespreventioncontrol-150620153942-lva1-app6892/95/diabetes-prevention-control-3-638.jpg?cb=1434815503
12. Bressler NM. Age-related macular degeneration is the leading cause of blindness. JAMA 2004;291:1900–1.

13. Wet AMD Image [Online] Available at: https://www.healios.co.jp/images/step_3_e.png
14. T. J. Wolfensberger, A. M. Hamilton “Diabetic retinopathy – An historical review”, Seminars on ophthalmology 2001, volume 16, issue 1.
15. Macular degeneration Image [Online] Available at: http://www.abc.es/media/salud/2017/06/02/DMAE-kzGB--620x349@abc.jpg
16. Fundus image [Online] Available at: https://i.pinimg.com/originals/2b/16/65/2b16658d91b0d769cc24a9393930fbf3.jpg
17. Image [Online] Available at: https://www.opsweb.org/resource/resmgr/op_fundus/fig2x02d.jpg
18. Internal structure of fundus camera Image [Online] Available at: https://encrypted-tbn0.gstatic.com/images?q=tbn:ANd9GcSfPHz2yG8XZ0ufrg1m4znEhmgE0xvNXs8wDA1BOWOrqHq6868k
19. Delori FC, Dorey CK, Staurenghi G, Arend O, Goger DG, Weiter JJ. “In vivo fluorescence of the ocular fundus exhibits retinal pigment epithelium lipofuscin characteristics.” Invest Ophthalmol Vis Sci. 1995;36(3):718–29.
20. Funds auto florescence imaging, Image [Online] Available at: https://www.opsweb.org/resource/resmgr/op_fundus/faf4.jpg
21. Huang D, Swanson EA, Lin CP, Schuman JS, Stinson WG, Chang W, Hee MR, Flotte T, Gregory K, Puliafito CA, Fujimoto JG.” Optical coherence tomography”. Science. 1991;254:1178–1181
22. Tearney GJ, Bouma BE, Boppart SA, Golubovic B, Swanson EA, Fujimoto JG. “Rapid acquisition of *in vivo* biological images by use of optical coherence tomography”. Opt Lett. 1996;21:1408–1410.
23. Advances in super-resolution imaging, applications in biology and medicine Image [Online] Available at: https://www.researchgate.net/profile/Maria_Hernandez42/publication/313553790/figure/fig1/AS:463891764387843@1487611823828/Microscope-history-timeline-and-the-application-of-the-super-resolution-technology-in.jpg
24. Tearney GJ, Bouma BE, Fujimoto JG. “High-speed phase- and group-delay scanning with a grating-based phase control delay line”. Opt Lett. 1997;22:1811–1813.
25. Bouma B, Tearney GJ, Boppart SA, Hee MR, Brezinski ME, Fujimoto JG. “High-resolution optical coherence tomographic imaging using a mode-locked Ti-Al_2O_3 laser source”. Opt Lett. 1995;20:1486–1488.

26. Tearney GJ, Boppart SA, Bouma BE, Brezinski ME, Weissman NJ, Southern JF, Fujimoto JG. “Scanning single-mode fiber optic catheter-endoscope for optical coherence tomography”. Opt Lett.1996;21:912–912.
27. Boppart SA, Bouma BE, Pitris C, Tearney GJ, Fujimoto JG, Brezinski ME. “Forward-imaging instruments for optical coherence tomography”. Opt Lett. 1997;22:1618–1620.
28. 3D OCT camera Image [Online] Available at: http://www.device.com.au/wp-content/themes/custom/js/timthumb.php?src=http://www.device.com.au/wp-content/uploads/2013/03/maestro.jpg&w=460&h=345
29. Leyuan Fang, Shutao Li, Qing Nie, Joseph A. Izatt, Cynthia A. Toth, and Sina Farsiu, “Sparsity based denoising of spectral domain optical coherence tomography images” biomedical optics express, May 2012, Vol. 3, No. 5, 942.
30. Damber Thapa, Kaamran Raahemifarc and Vasudevan Lakshminarayanan, “Reduction of speckle noise from optical coherence tomography images using multi-frame weighted nuclear norm minimization method” Journal of Modern Optics, 2015, Vol. 62, No. 21, 1856–1864
31. Gu, S. Zhang, L. Zuo, W. and Feng, X. “Weighted Nuclear Norm Minimization and Its Applications to Low Level Vision” In IEEE Conference on Computer Vision and Pattern Recognition, Columbus, OH, 2014.
32. H. Takeda, S. Farsiu, and P. Milanfar, “Kernel regression for image processing and reconstruction,” IEEE Trans. Image Process. 16, 349–366 (2007).
33. H. Takeda, S. Farsiu, and P. Milanfar, “Deblurring Using Regularized Locally Adaptive Kernel Regression,” IEEE Trans. Image Process. 17(4), 550–563 (2008).
34. H. J. Seo and P. Milanfar, “Training-Free, Generic Object Detection Using Locally Adaptive Regression Kernels,” IEEE Trans. Pattern Anal. Mach. Intell. 32(9), 1688–1704 (2010).
35. Tsechpenakis G, Lujan B, Martinez O, Gregori G, Rosenfeld PJ “Geometric Deformable Model Driven by CoCRFs: Application to Optical Coherence Tomography”, International Conference on Medical Image Computing and Computer Assisted Intervention, 2008.
36. F. A. Medeiros, L. M. Zangwill, C. Bowd, R. M. Vessani, R. Susanna, Jr., and R. N. Weinreb, “Evaluation of retinal nerve fiber layer, optic nerve head, and macular thickness measurements for glaucoma detection using optical coherence tomography,” Am. J. Ophthalmol, January 2005, Volume 139, Issue 1, 44–55
37. S. Farsiu, S. J. Chiu, R. V. O’Connell, F. A. Folgar, E. Yuan, J. A. Izatt, and C. A. Toth, “Quantitative Classification of Eyes with and without Intermediate Age-related Macular Degeneration Using Optical Coherence Tomography,” Ophthalmology,2005, Volume **121**, 162–172

38. G. Gregori, F. Wang, P. J. Rosenfeld, Z. Yehoshua, N. Z. Gregori, B. J. Lujan, C. A. Puliafito, and W. J. Feuer, "Spectral domain optical coherence tomography imaging of drusen in nonexudative age-related macular degeneration," Ophthalmology **118**(7), 1373–1379 (2011).
39. R. Koprowski, S. Teper, Z. Wróbel, and E. Wylegala, "Automatic analysis of selected choroidal diseases in OCT images of the eye fundus," Biomed. Eng. Online **12**(1), 117 (2013).
40. Y. Zhang, B. Zhang, F. Coenen, J. Xiao, and W. Lu, "One-class kernel subspace ensemble for medical image classification," EURASIP J. Adv. Signal Process. **2014**, 1–13 (2014).
41. Richard F Spaide, "Improving the age related macular degeneration construct: A new classification system," Retina, 38(5), 891-899 (2018).
42. P. P. Srinivasan, S. J. Heflin, J. A. Izatt, V. Y. Arshavsky, and S. Farsiu, "Automatic segmentation of up to ten layer boundaries in SD-OCT images of the mouse retina with and without missing layers due to pathology," Biomed. Opt. Express **5**(2), 348–365 (2014).
43. World's largest annotated SD-OCT dataset for intermediate AMD and control subjects [online] available at: http://people.duke.edu/~sf59/software.html